Supplementary Appendix

This appendix has been provided by the authors to give readers additional information about their work.

Supplement to: Wang P-Y, Ma W, Park J-Y, et al. Increased oxidative metabolism in the Li–Fraumeni syndrome. N Engl J Med 2013;368:1027-32. DOI: 10.1056/NEJMoa1214091

Supplementary Appendix

Supplement to: Wang, P-y, et al.

Increased Oxidative Metabolism in the Li-Fraumeni Syndrome

Contents

Supplementary Methods

TP53 genetic testing centers for the LFS family members

1) Genetic Diagnostic Laboratory, Department of Genetics, University of Pennsylvania School of Medicine, Philadelphia, PA

2) Clinical Molecular Diagnostic Laboratory, City of Hope National Medical Center, City of Hope, Duarte, CA

3) Clinical Cancer Genetics, MD Anderson Cancer Center, Houston, TX

4) DNA Diagnostic Laboratory, Baylor College of Medicine, Houston, TX

5) Quest Diagnostics Nichols Institute, San Juan Capistrano, CA

6) Molecular Genetics Lab, British Columbia Cancer Agency, Vancouver, Canada

7) Molecular Oncology and Cancer Genetics Laboratory, Huntington Medical Research Institutes, Pasadena, CA

Phosphorus-31 magnetic resonance spectroscopy of skeletal muscle

The tibialis anterior muscle of the supine subject was studied at 7.5 sec time resolution in a 3-T MRI scanner (GE Healthcare, Waukesha, WI). A 3-inch diameter ^{31}P surface coil was placed over the tibialis anterior muscle, about one-third the distance from the origin of the tibialis anterior muscle (lateral condyle) to the medial malleolus of the dominant leg. Submaximal exercise was performed by dorsiflexing (~40 times over 2 min) against an adapted custom-built pedal that was attached via a pulley system to 30% of the maximum lifted weight by the subject [1]. ^{31}P spectra were continuously obtained at rest, during exercise and recovery for 3 min, 2 min and 6 min, respectively. The spectra were acquired using a non-selective RF pulse (184 μs

duration, 2500 Hz spectral width, 2048 data points, 1.25 s repetition time and 6 excitations) and processed with 5 Hz line broadening, zero filling, Fourier transformation and baseline and phase corrections. PCr peak amplitudes during the recovery period were determined by lineshape analysis. The average PCr lineshape during 2.5 - 3.75 min of the recovery period was used as the model lineshape. Post-exercise PCr amplitudes (7.5 s – 3.725 min, 29 data points) were fitted to a single exponential curve and used to calculate the PCr recovery time constant (T_c) [2]. Spectral processing, lineshape analysis and curve fitting were performed using SAGE 7 (GE Healthcare) and IDL (version 6.4, Exelis Visual Information Solutions) software.

Metabolic exercise stress testing and oxygen consumption at ventilatory threshold

Symptom-limited metabolic (cardiopulmonary) exercise stress testing was performed on a treadmill with a conservative ramping protocol to determine peak oxygen consumption (VO_2) at ventilatory threshold [3]. Through the use of a metabolic cart (Vmax Spectra 229C, Sensormedics, Yorbal Linda, CA), minute ventilation, VO_2, and carbon dioxide output were acquired breath-by-breath, and averaged over 10-second intervals. The metabolic cart was calibrated according to manufacturer specifications prior to each test. VO_2 at ventilatory threshold was determined by the ventilatory equivalents method [4].

Cell culture

Primary human skeletal muscle myoblasts were isolated from vastus lateralis muscle needle biopsy specimens, treated with trypsin/collagenase and cultured in DMEM (GlutaMax-I, Invitrogen) supplemented with 20% FBS and 2 μM uridine [5]. Human lymphocytes were

prepared as previously described [6]. Briefly, peripheral blood mononuclear cells (PMBCs) were collected by density centrifugation using citrate-containing Vacutainer CPT tubes (Becton Dickinson). PMBCs were activated on immobilized anti-CD3 and anti-CD28 antibodies for 3 days and subsequently cultured in RPMI media supplemented with IL-2 (10 U/ml). 3 x 10^5 T cells were seeded in XF-96 plates coated with Cell-Tak and analyzed as described [7]. Mouse embryo fibroblasts (MEF) were isolated from 13.5 to 14.5-day embryos using standard protocols [8].

Mice

All mice were maintained and handled in accordance with the NHLBI Animal Care and Use Committee. The p53 R172H mouse (strain 01XL9, NCI Frederick Mouse Repository [9]) was backcrossed at least five generations into a C57BL/6 background. All mice were healthy, tumor-free male, age-matched at ~10-11 wk unless stated otherwise.

Mouse exercise and metabolic testing

Approximately 10 wk-old male mice were used for the treadmill exercise test as described previously [8]. While concurrently monitoring food intake and activity, indirect calorimetry was used to measure basal metabolism after a 2 d minimum period of acclimation (Columbia Instruments). Light and dark cycles of the day were 12-hr periods starting at 6 am and 6 pm, respectively. The data presented are the average of two 12-hr periods for each group of mice.

Mitochondrial studies

Mitochondria were isolated from tissues using standard techniques [10]. The Seahorse XF metabolic analyzer (Seahorse Bioscience) or Clark-type oxygen microelectrode was used for either whole cell or isolated mitochondrial oxygen consumption studies at 37°C as previously described [8, 10, 11]. Trifluorocarbonylcyanide phenylhydrazone (FCCP) at 1 μM concentration was used to measure uncoupled respiration.

Protein western blotting

Protein samples were solubilized in cold lysis buffer with protease inhibitor cocktail (Roche), resolved by Tris-glycine SDS PAGE, and transferred to Immobilon-P membrane (Millipore) for standard ECL western blotting.

mRNA quantification by real-time RT-PCR

RNA was isolated from tissue culture cells by solubilizing in lysis buffer using the poly(dT) magnetic bead system (Invitrogen), reverse transcribed using Superscript II (Invitrogen), and quantified by real-time polymerase chain reaction using SYBR green fluorescence on a 7900HT Sequence Detection System (Applied Biosystems) (RT-PCR) [12].

List of antibodies

Antibodies used were as follows: Mouse monoclonal anti-p53 (DO-1) and anti-actin (Santa Cruz); rabbit polyclonal anti-SCO2 [13]; anti-human TFAM (Abcam); rabbit polyclonal anti-mouse TFAM (a generous gift from Dr. Eric A. Shoubridge, McGill University); mouse monoclonal anti-mitochondrial MTCO1, MTCO2, SDHA, NDUFA 9, VDAC1 (Molecular Probes); rabbit

polyclonal anti-BAX (Cell Signaling); mouse monoclonal anti-p21 (Calbiochem); mouse monoclonal anti-tubulin (Clone B-5-1-2, Sigma).

List of real-time PCR primer sequences for mRNA analysis

mRNA quantification primers:

Mouse:
SCO2
F 5'-CAGCCTGTCTTCATCACTGTGGA
R 5'-GACACTGTGGAAGGCAGCTATGTGCC

TFAM
F 5'-CTGATGGGTATGGAGAAGGAGG
R 5'-CCAACTTCAGCCATCTGCTCTTC

p21
F 5'-AGGGCAACTTCGTCTGGGAG
R 5'-TTGGAGACTGGGAGAGGGCA

TIF,
F 5'-CTGAGGATGTGCTGTCTGGGAA
R 5'-CCTTTGCCTCCACTTCGGTC

Table S1. Characteristics of LFS mutation carrier subjects

Subject	p53 amino acid change	LFS family	Age	Cancer history (age at diagnosis)	Chemo-therapy
1	R181C	1	50	None	No
2	R273H	2	39	Breast cancer (32)	Yes
3	L130P	3	33	Breast cancer (25); papillary thyroid cancer (31)	Yes
4	R181C	1	53	Melanoma (48); renal cell cancer (50)	No
5	R181C	1	60	None	No
6	R181C	1	38	None	No
7	R181C	1	50	None	No
8	R181C	1	45	Breast cancer (43)	Yes
9	R181C	1	19	None	No
10	P222L; R267W	4	43	None	No
11*	P72R	5	52	Dermatofibroma (25); breast cancer (27, 28)	Yes
12	Y220C; P72R	6	31	Adrenocortical carcinoma (7 mo); breast cancer (25)	Yes
13	122X	7	23	Breast cancer (20)	Yes
14	122X	7	20	Breast cancer (15)	Yes
15	122X	7	21	Jaw osteosarcoma (12); breast cancer (17,19)	Yes
16	R273H	8	26	None	No
17	214X	9	31	Breast cancer (25)	Yes
18	R283C	10	29	None	No
19	R342X	11	33	Breast cancer (26)	Yes
20	R342X	11	56	Foot fibrosarcoma (3); prostate cancer (52)	No

*Subject 11 also had *TP53* non-coding sequence changes (IVS2+3 C->G; IVS5+1 G->A) reported to be associated with LFS [14].

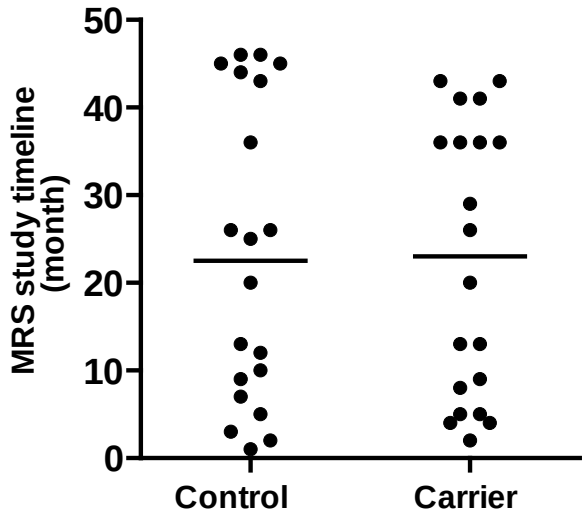

Figure S1. The MRS study timeline for control and LFS mutation carrier subjects. The date of the first scanned subject was designated as month one. The horizontal lines indicate the median value for the control (n = 20) and carrier (n = 20) groups: 22.5 versus 23.0 months, respectively. p = 0.75 by Mann-Whitney test.

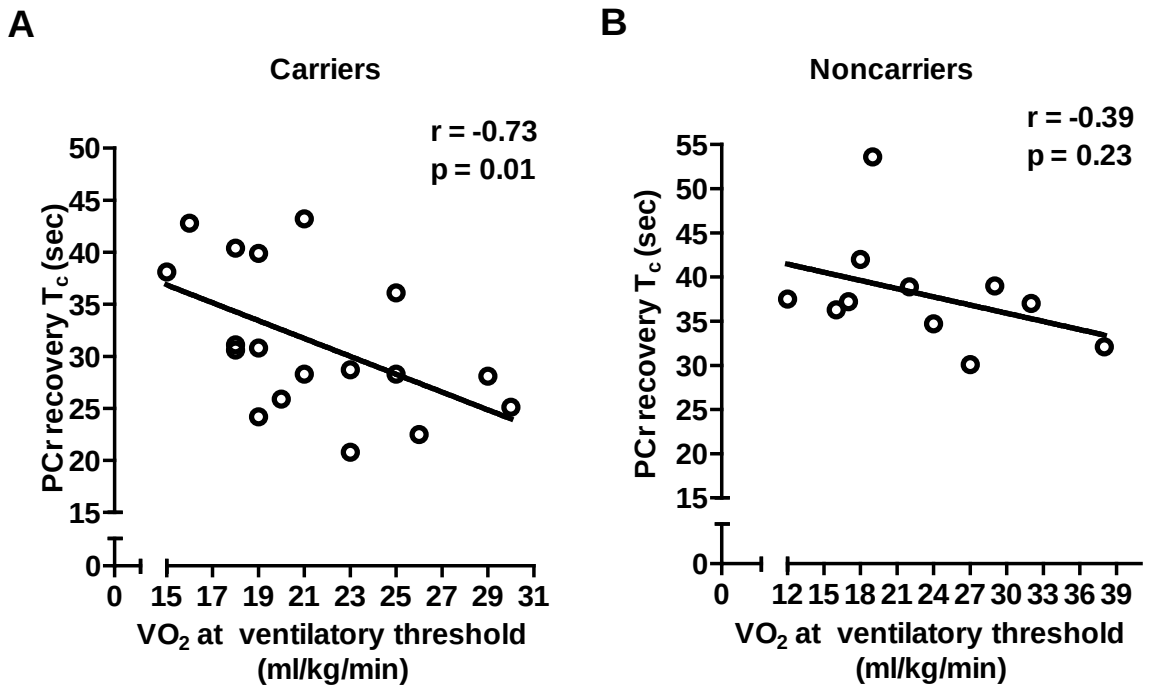

Figure S2. Correlation between PCr recovery time constant (T_c) and oxygen consumption in humans. (**A**) Individuals carrying LFS p53 mutations underwent cardiopulmonary exercise testing and their VO_2 at ventilatory threshold was determined as an index of submaximal aerobic endurance. Out of the 20 carrier subjects, two subjects were excluded from this analysis because of one individual with a leg amputation and another with severe obesity. Statistical analysis was performed using the two-tailed Pearson correlation coefficient method (n = 18). (**B**) Correlation between PCr T_c and VO_2 at ventilatory threshold in non-carrier LFS family members. This correlation did not reach significance likely due to the smaller number of control subjects who underwent metabolic exercise testing (n = 11).

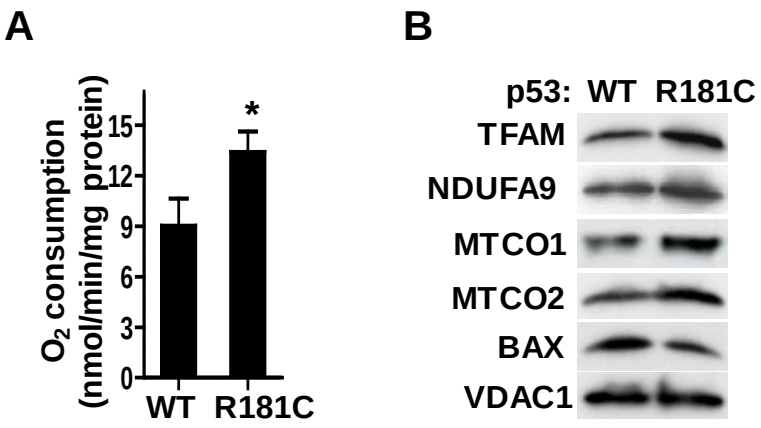

Figure S3. Increased oxygen consumption and mitochondrial biogenesis in human myoblasts harboring the *TP53* R181C mutation. (**A**) Oxygen consumption of 7 pairs of carrier (R181C) and non-carrier (WT) myoblasts from the same LFS family using a standard Clark-type oxygen electrode. (**B**) Mitochondria were isolated from pooled myoblasts of carrier or non-carrier family members and immunoblotted with the indicated antibodies. The lower level of BAX protein serves as a control for the R181C mutation as it has previoulsy been shown to display loss of apoptotic activity (IARC TP53 database). Values shown as mean $\pm$ SEM, *$p < 0.05$.

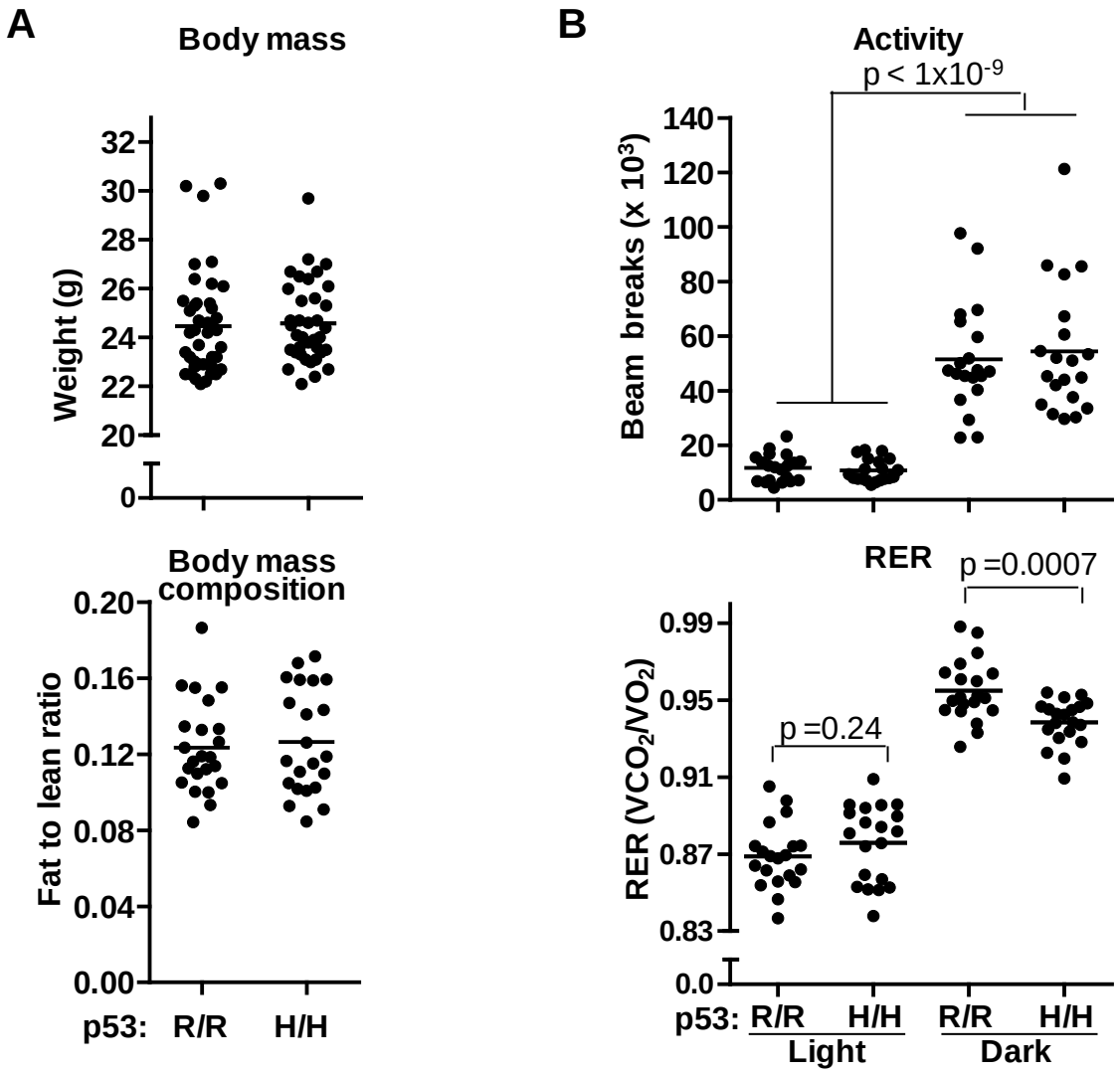

Figure S4. Metabolic characterization of the mouse model of LFS. (**A**) Body mass (g) of ~10 wk old male mice (n ≥ 37, p = 0.78) and body mass composition measured by NMR expressed as fat to lean ratio in 10 wk old male mice with two copies of the LFS mutation *p53* R172H (H/H) (homologous to human R175H) compared to wild-type mice (R/R) (n≥22, p=0.70). (**B**) Activity measured by beam breaks and respiratory exchange ratios (RER) during indicated cycle of the day (n = 20, ~10 wk old male mice). Light cycle, 6 am to 6 pm; dark cycle, 6 pm to 6 am. The horizontal lines indicate the mean value. p values for the activity between R/R and H/H mice were not significantly different. Both the activity and RER of the mice in the dark cycle are significantly different from that in the light cycle ($p < 1x10^{-9}$).

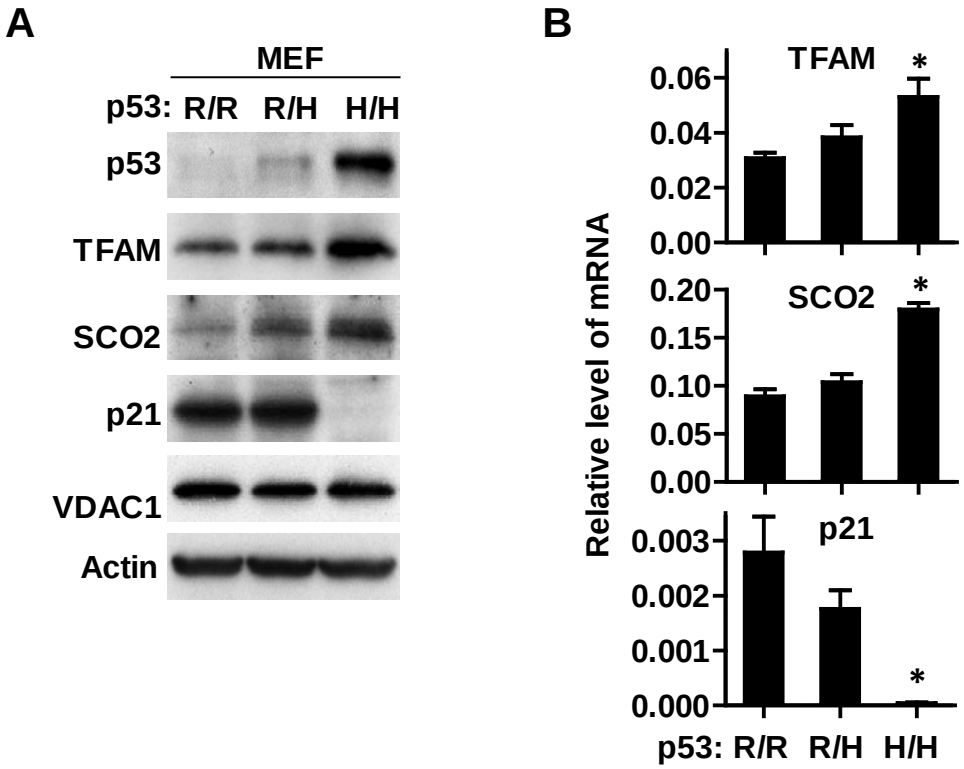

Figure S5. *p53* R172H mutation promotes mitochondrial biogenesis in mouse embryo fibroblasts (MEF). (**A**) Immunoblots of MEF cell lysates. Actin and VDAC1 were used as protein loading controls for whole cell lysates and mitochondria, respectively. (**B**) Effect of *p53* R172H genotype on MEF mRNA levels of the indicated genes by RT-PCR (n = 4). Note that p21 mRNA levels serve as a control to show loss of wild-type p53 transcriptional activity by the *p53* R172H mutation. The bars represent mean $\pm$ SEM. * $p < 0.05$ compared to wild-type (R/R).

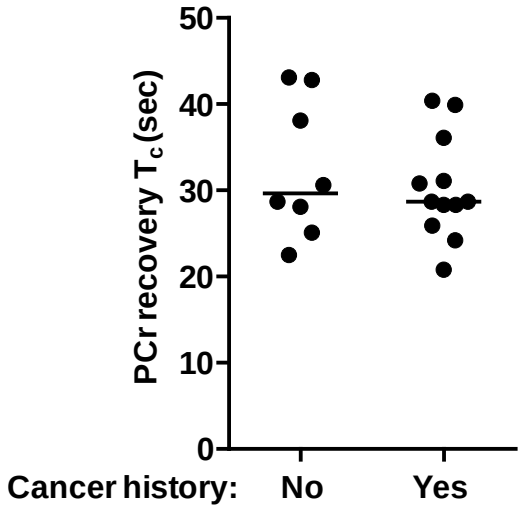

Figure S6. Comparison of PCr recovery T_c of LFS mutation carriers with or without past medical history of cancer. Of the 12 individuals with cancer history, 10 had also received chemotherapy (Table S1). The horizontal lines indicate the median value. p = 0.73 by Mann-Whitney test.

Supplementary References

1. Sheehan FT, Seisler AR, Siegel KL. In vivo talocrural and subtalar kinematics: a non-invasive 3D dynamic MRI study. Foot Ankle Int 2007;28:323-35.
2. Argov Z, Lofberg M, Arnold DL. Insights into muscle diseases gained by phosphorus magnetic resonance spectroscopy. Muscle Nerve 2000;23:1316-34.
3. Arena R, Humphrey R, Peberdy MA, Madigan M. Predicting peak oxygen consumption during a conservative ramping protocol: implications for the heart failure population. J Cardiopulm Rehabil 2003;23:183-9.
4. Balady GJ, Arena R, Sietsema K, et al. Clinician's Guide to cardiopulmonary exercise testing in adults: a scientific statement from the American Heart Association. Circulation 2010;122:191-225.
5. Yasin R, Van Beers G, Nurse KC, Al-Ani S, Landon DN, Thompson EJ. A quantitative technique for growing human adult skeletal muscle in culture starting from mononucleated cells. J Neurol Sci 1977;32:347-60.
6. Jackson SH, Devadas S, Kwon J, Pinto LA, Williams MS. T cells express a phagocyte-type NADPH oxidase that is activated after T cell receptor stimulation. Nat Immunol 2004;5:818-27.
7. van der Windt GJ, Everts B, Chang CH, et al. Mitochondrial respiratory capacity is a critical regulator of CD8+ T cell memory development. Immunity 2012;36:68-78.
8. Park JY, Wang PY, Matsumoto T, et al. p53 improves aerobic exercise capacity and augments skeletal muscle mitochondrial DNA content. Circ Res 2009;105:705-12, 11 p following 12.
9. Lang GA, Iwakuma T, Suh YA, et al. Gain of function of a p53 hot spot mutation in a mouse model of Li-Fraumeni syndrome. Cell 2004;119:861-72.
10. Frezza C, Cipolat S, Scorrano L. Organelle isolation: functional mitochondria from mouse liver, muscle and cultured fibroblasts. Nat Protoc 2007;2:287-95.
11. Zhang J, Nuebel E, Wisidagama DR, et al. Measuring energy metabolism in cultured cells, including human pluripotent stem cells and differentiated cells. Nat Protoc 2012;7:1068-85.
12. Patino WD, Mian OY, Kang JG, et al. Circulating transcriptome reveals markers of atherosclerosis. Proc Natl Acad Sci U S A 2005;102:3423-8.
13. Matoba S, Kang JG, Patino WD, et al. p53 regulates mitochondrial respiration. Science 2006;312:1650-3.
14. Hsu HC, Huang AM, Lai PL, Chien WM, Peng SY, Lin SW. Genetic alterations at the splice junction of p53 gene in human hepatocellular carcinoma. Hepatology 1994;19:122-8.